Preparation of VB-a/POSS Hybrid Monomer and Its Polymerization of Polybenzoxazine/POSS Hybrid Nanocomposites

Jieh-Ming Huang,[1] Shiao-Wei Kuo,[2] Hui-Ju Huang,[1] Yu-Xiang Wang,[1] Yun-Ting Chen[1]

[1]*Department of Chemical and Materials Engineering, Vanung University, Chung-Li 32054, Taiwan*
[2]*Department of Materials and Optoelectronic Engineering, Center for Nanoscience and Nanotechnology, National Sun Yat-Sen University, Kaohsiung, Taiwan*

Received 22 February 2008; accepted 5 August 2008
DOI 10.1002/app.29124
Published online 10 October 2008 in Wiley InterScience (www.interscience.wiley.com).

ABSTRACT: A benzoxazine monomer (VB-a) containing an allyl groups was synthesized through the Mannich condensation of bisphenol A, formaldehyde, and allylamine (bisphenol-A and allylamine as VB-a). This monomer was then reacted with polyhedral oligomeric silsesquioxane (POSS) through hydrosilylation, followed by thermal curing to form poly(VB-a)/POSS hybrid nanocomposites. The curing behavior of the nanocomposites was monitored using Fourier transform infrared spectroscopy (FTIR), and their thermal and morphological properties were investigated through thermogravimetric analysis (TGA), dynamic mechanical analysis (DMA), and scanning electron microscopy. DMA revealed that the glass transition temperatures of the poly(VB-a)/POSS nanocomposites were higher than that of the pristine poly(VB-a), presumably because the POSS cages effectively hindered the motion of the polymer chains. TGA confirmed that the thermal degradation temperatures and char yields of the polybenzoxazines increased after incorporation of the POSS moieties. © 2008 Wiley Periodicals, Inc. J Appl Polym Sci 111: 628–634, 2009

Key words: polybenzoxazine; POSS; nanocomposite

INTRODUCTION

Polybenzoxazines are novel thermosetting polymers that possess many physical properties that are superior to those of traditional polymers, such as epoxy and phenolic resins. Polybenzoxazines can be prepared through Mannich condensations of phenol, formaldehyde, and primary amines.[1–3] In addition, polybenzoxazines can be cured without the use of a strong acidic or basic catalyst under conditions that do not produce toxic gases or other byproducts. Polybenzoxazines have many outstanding performance features, such as low flammability, high thermal stability, low surface free energy, and low dielectric properties.[4,5] The glass transition temperature (T_g) of a typical polybenzoxazine-one prepared from a monomer having a difunctional oxazine ring (B-a) is 180°C, with a degradation temperature of $\sim$ 310°C.[6] To further enhance the performance of polybenzoxazines, much effort has been exerted into the preparation of polybenzoxazine alloys and copolymers.[7–23] For example, polymerizable acetylene side groups have been introduced into the benzoxazine monomer in an effort to improve the thermal stability of polybenzoxazines.[24,25] These acetylene-functionalized benzoxazines can be polymerized into three-dimensional networks exhibiting high thermooxidative stability and resistance to both solvent and moisture. If they are to be employed as high-performance materials, however, the thermomechanical properties of polybenzoxazines require further enhancement to widen their applicability. Recently, novel classes of organic/inorganic hybrid materials have been developed based on polyhedral oligomeric silsesquioxane (POSS),[26–33] a cubic form of silica that is rigid, has defined dimensions (0.53 nm), and presents eight organic groups (functional or inert) at the vertices of the cube. POSSs derivatives have several advantages over conventional inorganic fillers, including monodispersity, low density, high thermal stability, and controllable functionalities. In addition, POSS monomers can be directly blended with polymers or copolymerized with other monomers to form polymer/POSS nanocomposites. Dispersing an inorganic POSS component uniformly within an organic polymer matrix at the nanoscale level can have a synergistic effect on improving the bulk properties.[34–36] Several nanocomposite hybrid polymers incorporating POSS exhibit increased values of their glass transition (T_g), and decomposition (T_{dec}) temperatures,

Correspondence to: J.-M. Huang (jiehming@msa.vnu.edu.tw).

Contract grant sponsor: National Science Council, Taiwan, Republic of China; contract grant numbers: NSC-93-2216-E-238-002, NSC-94-2216-E-238-003.

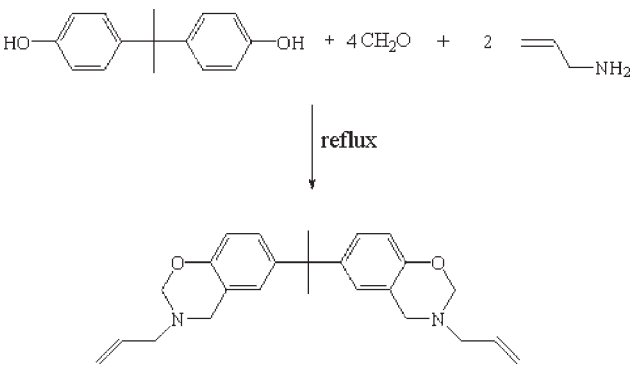

Scheme 1 Synthesis of the VB-a benzoxazine monomer.

improved resistance to oxidation, and reduced flammability.[37–39] Nevertheless, polybenzoxazine/POSS nanocomposites have been reported in only a few articles to date.[40–45] Previously, we reported the properties of polybenzoxazine/POSS hybrids synthesized through solution blending of a benzoxazine monomer with either H-POSS or isobutyl-POSS.[46] Disappointingly, because of poor miscibility, the IB-POSS-modified polybenzoxazine hybrids had values of T_g lower than that of the pure polybenzoxazine. In this article, we report the synthesis of poly(VB-a)/POSS hybrid nanocomposites through hydrosilylation of an allyl-terminated benzoxazine with POSS, and discuss their morphologies and thermal properties. These nanocomposites containing POSS moieties in a polybenzoxazine matrix possess noticeably improved thermal stability, as revealed through thermogravimetric analysis (TGA) and dynamic mechanical analysis (DMA).

EXPERIMENTAL

Materials

Octakis(dimethylsilyloxy)silsesquioxane (HMe_2SiO-$SiO_{1.5})_8$, $Q_8M_8^H$, platinum 1,3-divinyl-1,1,3,3-tetramethyldisiloxane [Pt(dvs)], aqueous formaldehyde solution (37%), allylamine, and bisphenol A were purchased from Aldrich Chemical (USA). To prepare the polybenzoxazine/POSS nanocomposite, a vinyl-terminated benzoxazine monomer (VB-a) was synthesized according to the procedure outlined in Scheme 1.[47] An aqueous formaldehyde solution (16.5 g) and bisphenol A (11.4 g) were mixed with methyl ethyl ketone (50 mL) in a 250-mL three-necked flask. The mixture was cooled in an ice bath and then allylamine (11.4 g) was added dropwise using a dropping funnel. After an additional 30 min of stirring, the mixture was warmed gradually up to 80°C and then it was heated under reflux for 3 h. The solvent and water were evaporated *in vacuo*, and the residue was dissolved in ethyl ether (100 mL). The solution was washed several times with water and 2*N* aqueous NaOH to remove any impurities and unreacted monomers. The ether solution was then dried with sodium sulfate and the solvent evaporated at room temperature. The product was obtained as a light-yellow solid (23.5 g).

Preparation of VB-a/POSS hybrid monomer

The synthesis of the VB-a/POSS hybrids is presented in Scheme 2. The POSS derivative (HMe_2SiO-$SiO_{1.5})_8$ (1.018 g, 1 mmol) and toluene (10 mL) were stirred magnetically in a 25-mL Schlenk flask. The monomer VB-a (3.12 g, 8 mmol) was added, followed by 10 drops of 2.0 m*M* Pt(dvs). The reaction mixture was stirred for 8 h at 80°C, cooled, and then dry activated charcoal was added. After stirring for 10 min, the mixture was filtered through a 0.45-μm Teflon membrane. The solvent was evaporated to yield an opaque viscous liquid. The hybrid was poured onto an aluminum plate, dried for 6 h in the open air, placed in an oven, and then heated *in vacuo* at 50°C for 2 h. The hybrid monomer was poured into a stainless-steel mold and polymerized

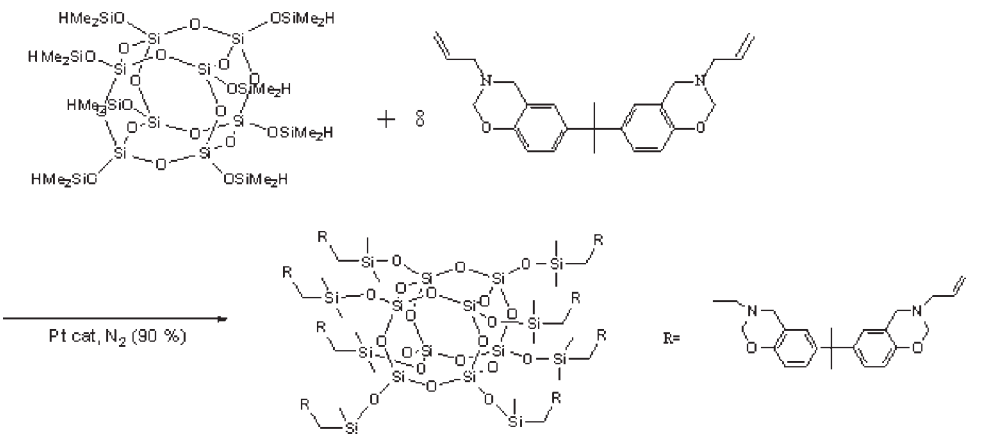

Scheme 2 Synthesis of the (VB-a)/POSS hybrid nanocomposites.

in a stepwise manner, heating at 120, 140, 160, and 200°C, for 2 h each. The product was then postcured at 220 and 240°C for 30 min each.

Proton nuclear magnetic resonance spectroscopy

^{1}H-NMR spectra were recorded using a Bruker DPX-300 spectrometer operated at 300 MHz, with $CDCl_3$ as the solvent at 298 K. The relaxation time was 2 s. Chemical shifts are reported in parts per million. Spectrometer operating at a resonance frequency is 300 and 75 MHz for ^{1}H and ^{13}C spectroscopy, respectively. TMA was used as reference and an acquisition time of 30 ms with 2048 scans were used.

Fourier transform infrared spectroscopy

FTIR spectra were recorded using a Perkin–Elmer Spectra One FTIR spectrometer (Norwalk, CT). FTIR spectra of the polymer films were recorded from samples prepared using conventional NaCl disk methods. Thus, a tetrahydrofuran solution containing the hybrid was cast onto a NaCl disk, which was dried under conditions similar to those used for the bulk preparation. The films obtained in this manner were sufficiently thin to obey the Beer–Lambert law. IR spectra recorded at elevated temperatures were obtained by using a cell mounted inside the temperature-controlled compartment of the spectrometer.

Dynamic mechanical analysis

DMA measurements were performed using a TA Instruments DMA Q800 (DuPont) instrument operated in a single-cantilever bending mode over the temperature ranging from 30 to 350°C. Data acquisition and analysis of the storage modulus (G'), loss modulus (G''), and loss tangent (tan δ) were recorded automatically by the system. The heating rate and frequency were fixed at 2°C/min and 1 Hz, respectively. Samples for DMA experiments were prepared by molding. The sample dimensions were 3 cm × 0.8 cm × 0.2 cm.

Thermogravimetric analysis

TGA was performed using a Perkin–Elmer TGA7 thermogravimetric analyzer (Norwalk, CT) operated at a heating rate of 10°C/min from room temperature to 800°C under a nitrogen flow of 20 mL/min. The measurements were conducted using 6–10 mg of the samples. Plots of weight retention versus temperature were recorded.

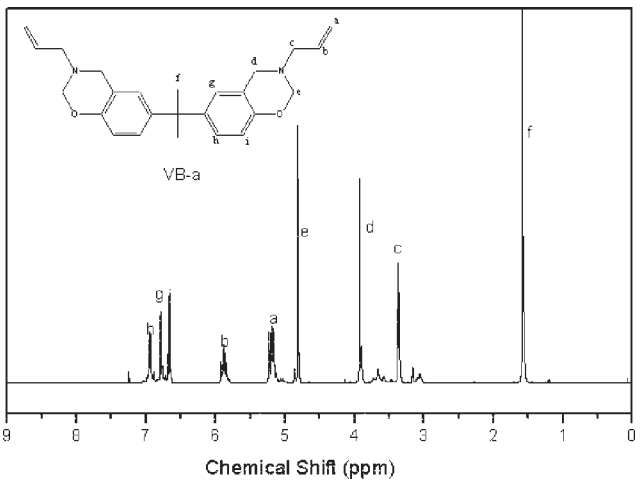

Figure 1 ^{1}H-NMR spectrum of VB-a.

Scanning electron microscopy

Samples of the poly(VB-a)/POSS hybrids were fractured cryogenically with liquid nitrogen. The morphologies of the cryogenically fractured surfaces of the specimens were examined under a Hitachi S-4700I scanning electron microscope. The fractured surfaces of the samples were coated with thin layers of Pt (∼ 3 nm).

RESULTS AND DISCUSSION

Characterization of VB-a

Figure 1 displays the ^{1}H-NMR spectrum of the vinyl-terminated benzoxazine (VB-a) monomer. The vinyl group appears as two resonances, at 5.21 and 5.88 ppm, in a 2 : 1 ratio. We assign the peaks at 3.9 and 4.8 ppm to protons in the methylene bridge of the oxazine. The signal of the protons located between the vinyl group and the nitrogen atom appears at 3.37 ppm. The peaks at 1.57 and 6.66–6.96 ppm are attributed to the $C(CH_3)_2$ and aromatic protons, respectively. Figure 2 presents the ^{13}C-NMR spectrum of VB-a. The signals of the carbon atoms of the terminal olefin unit appear at 116 and 138 ppm. We assign the characteristic signals at 52 and 82 ppm to the carbon atoms of the oxazine ring. These NMR spectra confirmed that we had successfully synthesized VB-a. Figure 3 displays FTIR spectra of poly(VB-a) and the poly(VB-a)/POSS hybrid nanocomposites. We observe the characteristic absorptions of the benzoxazine at 1230 (asymmetric stretching of C—O—C units) and 1498 (attributable to the 1,2,4-trisubstituted benzene ring) cm^{-1}.[1] The characteristic absorption bands of the allyl group appear at 3075 (=C—H stretching) and 1644 (of C=C stretching) cm^{-1}. All of these features are indicative of the presence of vinyl-terminated benzoxazine groups. In Figure 3(b), the absorption peak at

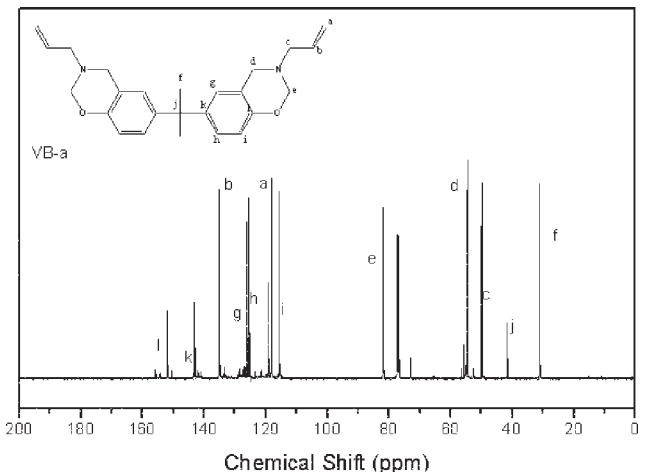

Figure 2 ^{13}C-NMR spectrum of VB-a.

2144 cm^{-1} corresponding to Si—H stretching vibrations was almost disappeared, and the absorption peak at 1100 cm^{-1} was observed indicating that the hydrosilylation of VB-a/POSS was synthesized successful.

Curing and polymerization of the VB-a/POSS hybrids

The formation of silicon–carbon bonds is one of the best ways to exploit organosilicon chemistry to create new organic/inorganic materials. Hydrosilylation refers to the addition of a Si—H unit across an unsaturated bond, such as C=C or C≡C units.[48] The hydrosilylation of an olefin results in a saturated hydrocarbon; it can be accomplished through either a free radical process or the use of transition metal catalysts.[49,50] In this study, we used Pt(dvs) as a catalyst to synthesize the allylamine-terminated benzoxazine POSS (VB-a/POSS), which we then subjected to a free radical hydrosilylation. Figure 4 displays

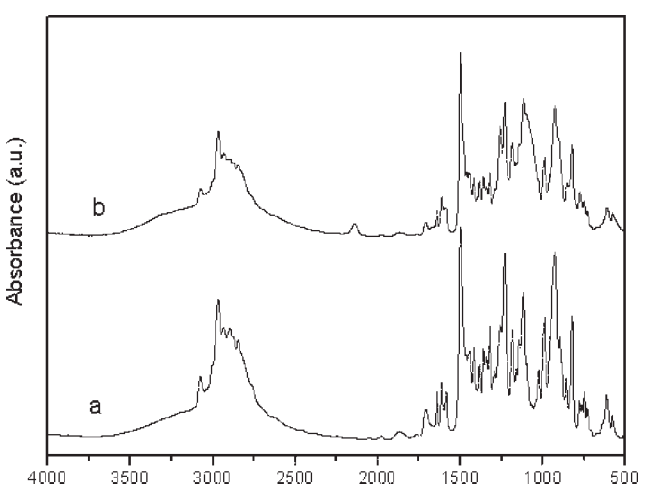

Figure 3 FTIR spectra of (a) poly(VB-a) and (b) the poly (VB-a)/POSS hybrid nanocomposites.

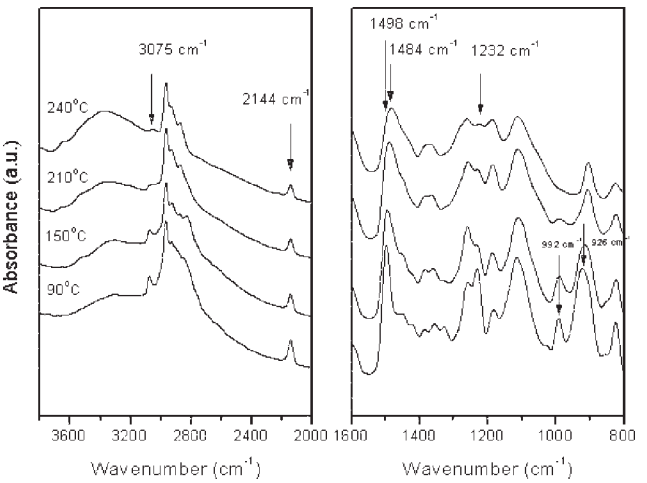

Figure 4 FTIR spectra of VB-a/POSS hybrid nanocomposites cured at various temperatures for 2 h.

FTIR spectra of the VB-a/POSS hybrids cured at different temperatures (90, 150, 210, and 240°C) for 2 h. The significant decrease in the intensities of the bands at 926 and 1232 cm^{-1}, which indicate the presence of benzoxazine ring,[51–53] implies that ring opening reactions had occurred. In addition, a new band for the tetra-substituted aromatic ring of the polymerized VB-a appears at 1484 cm^{-1}, with a corresponding decrease in the intensity of the band representing the tri-substituted aromatic ring of VB-a (1498 cm^{-1}). We followed the conversion of the vinyl groups in the VB-a monomer by monitoring of the change in the intensity of the band at 3075 cm^{-1}, which is associated with C—H stretching of the vinyl group. Although the signal at 2144 cm^{-1} (Si—H stretching) decreased upon increasing the curing temperatures, it still remained even after curing at 240°C for 2 h, suggesting that the hydrosilylation of VB-a did not reach completion because of steric

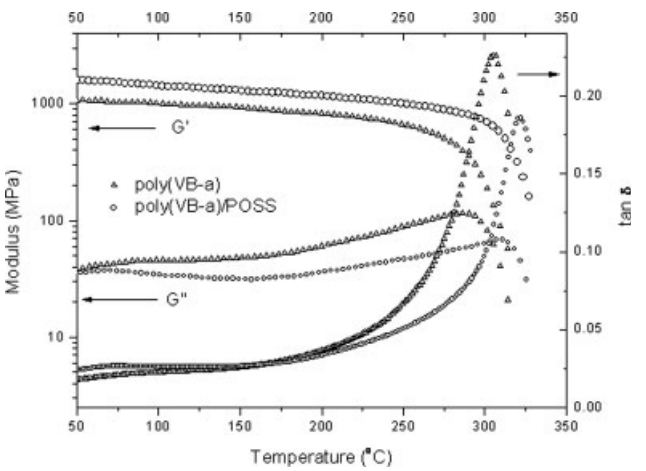

Figure 5 Storage modulus (G'), loss modulus (G''), and loss tangents (tan δ) of poly(VB-a) and the poly(VB-a)/POSS hybrid nanocomposites.

TABLE I
Thermal Properties of Poly(VB-a) and the Poly(VB-a)/POSS Nanocomposites

	DMA			TGA	
Sample	G' (MPa)[a]	G'' (°C)	tan δ (°C)	T_5 (°C)	Ash (%)[b]
Poly(VB-a)	1,086	289.4	301.2	347.2	22.3
Poly(VB-a)/POSS	1,576	310.7	324.3	355.6	45.9

[a] Measured at 50°C.
[b] Measured at 800°C.

hindrance around the POSS cages. Here, we could calculate the conversion of Si—H group ~ 30% by using the intensity ratio at 2144 cm^{-1} with the same band prior to hydrosilylation.

Dynamic mechanical analysis

We examined the viscoelastic properties of the polybenzoxazine along with the polybenzoxazine/POSS hybrid nanocomposites. Figure 5 displays the temperature dependence of the G', G'', and tan δ of poly(VB-a) and the poly(VB-a)/POSS nanocomposite; Table I summarizes the results. The G' for poly(VB-a) and the poly(VB-a)/POSS nanocomposite at 50°C were 1086 and 1576 MPa, respectively. From the G' curves, we clearly observe an increase in the modulus intensity after the inclusion of POSS into the hybrid. From the G'' curves, we observe a decreased peak intensity accompanying an upshift of the temperature position after the addition of POSS moieties into the polybenzoxazine matrix. A peak shift in the dynamic properties of a hybrid results primarily from strong interactions between its components. The POSS particles covalently bonded in the poly (VB-a) hybrid hindered the motion of the molecular chains to some extent; thus, a higher temperature was required for activation. From the maxima in the G'' curve, we determined the value of T_g of the poly (VB-a) to be ~ 289°C. For the poly(VB-a)/POSS hybrid nanocomposites, the corresponding value of T_g shifted to as high as 310°C. Thus, our analyses of the viscoelastic properties revealed that a noticeable increase in T_g (up to ~ 21°C) occurred for the vinylpolybenzoxazine, indicating that the nanometer-scale POSS cages could restrict the motion of the macromolecular chains in the hybrid nanocomposites. In addition, in the tan δ curves, we observe a slight depression of the peak intensity upon inclusion of the POSS cages. Because the damping property is provided by the ratio of the viscous and elastics components, we surmise that the reduced peak height was associated with a lower segmental mobility and fewer relaxation species; this behavior is indicative of a higher degree of crosslinking for the poly(VB-a)/POSS hybrid. Thus, we attribute the decreased magnitude of the α-relaxation peak of poly(VB-a) to the more extensive crosslinking that occurred after POSS had been added into the hybrids.

Thermal stability of poly(VB-a) and poly(VB-a)/POSS nanocomposites

We used TGA to investigate the thermal stability of the polybenzoxazines and their hybrids containing POSS. Figure 6 displays the TGA thermograms of poly(VB-a) and the poly(VB-a)/POSS nanocomposites; Table I lists the pertinent data collected from the thermograms. The 5 and 10% weight loss temperatures (T_5 and T_{10}) for poly(VB-a) were 347.2 and 365.7°C, respectively, whereas for the poly(VB-a)/POSS nanocomposites, these values increased to 355.5 and 411.7°C, respectively. In addition, the char yield at 800°C of the poly(VB-a)/POSS nanocomposites was 45.9% much higher than that of poly(VB-a) (22.6%), i.e., char enrichment occurred after incorporation of POSS moieties into poly(VB-a). An increased char yield corresponds to a reduction in the evolution of volatiles during thermal degradation and a decrease in polymer flammability. These TGA results indicate the good thermal stability of the polybenzoxazine hybrids after the incorporation of POSS moieties led to the formation of an inorganic protection layer on the nanocomposite's

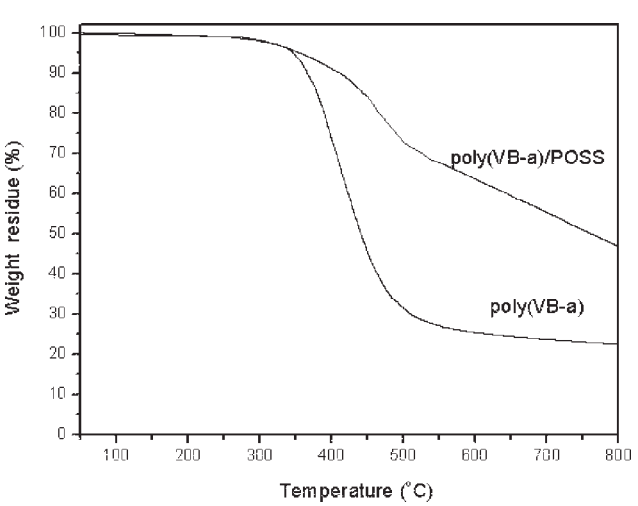

Figure 6 TGA thermograms of poly(VB-a) and the poly (VB-a)/POSS hybrid nanocomposites.

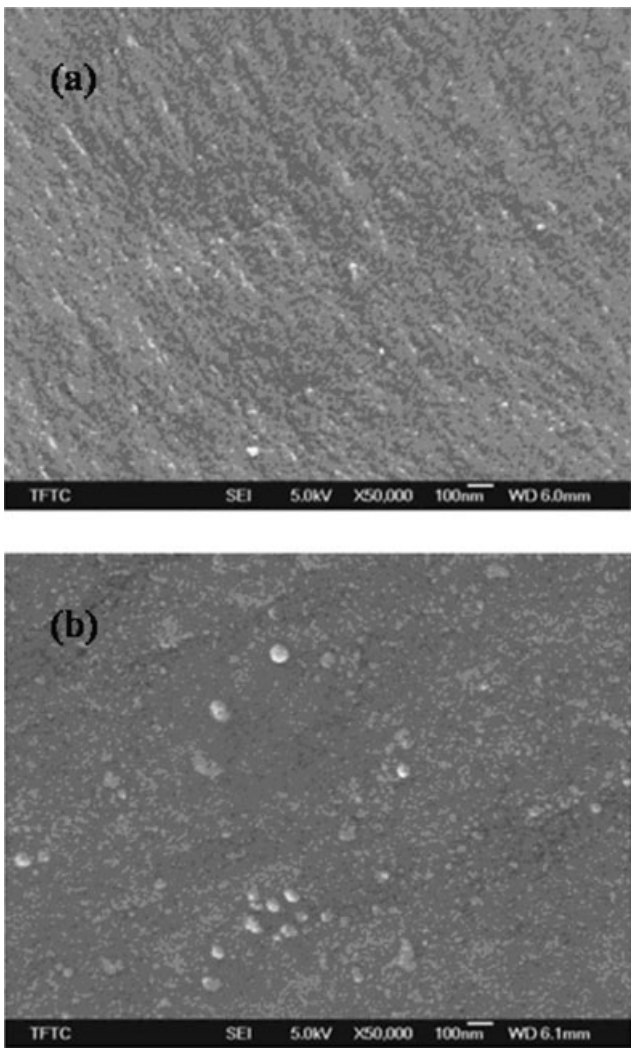

Figure 7 SEM cross-sectional micrographs of (a) the poly (VB-a)/POSS hybrid nanocomposites and (b) the 90/10 poly(VB-a)/POSS blend.

surface, which have been discussed in our previous study.[54]

Morphology of poly(VB-a)/POSS nanocomposites

We used scanning electron microscopy (SEM) to investigate the morphology of the poly(VB-a)/POSS hybrid nanocomposites. Figure 7 displays SEM cross-sectional images of the poly(VB-a)/POSS nanocomposites and the 90/10 poly(VB-a)/POSS blend prepared through solution blending of the VB-a monomer and 10 wt % of POSS in THF. The SEM micrograph of the poly(VB-a)/POSS nanocomposite [Fig. 7(a)] indicates that the POSS moieties remained evenly dispersed within the polybenzoxazine matrix. In comparison, the domain sizes in the 90/10 poly (VB-a)/POSS blend [Fig. 7(b)] were significantly larger than those in the poly(VB-a)/POSS nanocomposites. The 90/10 poly(VB-a)/POSS blend exhibits gross POSS aggregation arising from the weaker interactions and poorer miscibility between POSS and poly(VB-a). Because the poly(VB-a)/POSS hybrid nanocomposites were synthesized through hydrosilylation reactions, the covalent bonds formed between the VB-a and POSS units improved the miscibility dramatically. The diameters of the POSS particles in the poly(VB-a)/POSS hybrid nanocomposites were between 10 and 30 nm.

CONCLUSIONS

We have synthesized and characterized a vinyl-benzoxazine monomer (VB-a) featuring terminal vinyl groups and then used it to prepare poly(VB-a)/POSS hybrids through hydrosilylation with POSS, followed by thermal curing of the benzoxazine units to form poly(VB-a)/POSS hybrid nanocomposites. FTIR spectra indicated that not all of the Si—H groups reacted with VB-a, presumably because of the steric bulk of the POSS cages. The addition of POSS to the poly(VB-a) network greatly increased the crosslinking density and improved the thermal properties of the polymer. For example, the mechanical relaxation temperature increased from 301°C for poly(VB-a) to 324°C for the poly(VB-a)/POSS hybrid nanocomposite. The degradation temperature and char yield of the nanocomposite under nitrogen increased after the incorporation of POSS into the hybrid, implying that modifying polybenzoxazine through the incorporation of POSS cages improves the thermal stability of the nanocomposites.

References

1. Ning, X.; Ishida, H. J Polym Sci Part B: Polym Phys 1994, 32, 921.
2. Ning, X.; Ishida, H. J Polym Sci Part A: Polym Chem 1994, 32, 1121.
3. Ishida, H. U.S. Pat 5,543,516 (1996).
4. Wang, C. F.; Su, Y. C.; Kuo, S. W.; Huang, C. F.; Sheen, Y. C.; Chang, F. C. Angew Chem Int Ed 2006, 45, 2248.
5. Ishida, H.; Low, H. Macromolecules 1997, 33, 1099.
6. Ishida, H.; Allen, D. J Polym Sci Part B: Polym Phys 1996, 34, 1019.
7. Ishida, H.; Ohba, S. J Appl Polym Sci 2006, 101, 1670.
8. Ishida, H.; Ohba, S. Polymer 2005, 46, 5588.
9. Rimdusit, S.; Ishida, H. Polymer 2000, 41, 7941.
10. Agag, T.; Taepaisitphongse, V.; Takeichi, T. Polym Compos 2007, 28, 680.
11. Agag, T.; Tsuchiya, H.; Takeichi, T. Polymer 2004, 45, 7903.
12. Agag, T.; Takeichi, T. J Polym Sci Part A: Polym Chem 2007, 45, 1878.
13. Takeichi, T.; Guo, Y.; Rimdusit, S. Polymer 2005, 46, 4909.
14. Takeichi, T.; Zeidam, R.; Agag, T. Polymer 2002, 43, 45.
15. Takeichi, T.; Agag, T.; Zeidam, R. J Polym Sci Part A: Polym Chem 2001, 39, 2633.
16. Kimura, H.; Matsumoto, A.; Hasegawa, K.; Fukuda, A. J Appl Polym Sci 1999, 72, 1551.
17. Kimura, H.; Matsumoto, A.; Sugito, H.; Hasegawa, K.; Ohtsuka, K.; Fukuda, A. J Appl Polym Sci 2001, 79, 555.

18. Liu, Y. L.; Hsu, C. W.; Chou, C. I. J Polym Sci Part A: Polym Chem 2007, 45, 1007.
19. Liu, Y. L.; Yu, J. M. J Polym Sci Part A: Polym Chem 2006, 44, 1890.
20. Yei, D. R.; Fu, H. K.; Chen, W. Y.; Chang, F. C. J Polym Sci Part B: Polym Phys 2006, 44, 347.
21. Chen, Q. A.; Xu, R. W.; Yu, D. S. J Appl Polym Sci 2006, 100, 4741.
22. Rao, B. S.; Pathak, S. K. J Appl Polym Sci 2006, 100, 3956.
23. Rimdusit, S.; Tanthapanichakoon, W.; Jubsilp, C. J Appl Polym Sci 2006, 99, 1240.
24. Agag, T.; Takeichi, T. Macromolecules 2001, 34, 7257.
25. Kim, H. J.; Brunovska, Z.; Ishida, H. Polymer 1999, 40, 6565.
26. Haddad, T. S.; Lichtenhan, J. D. Macromolecules 1996, 29, 7302.
27. Xu, H.; Kuo, S. W.; Lee, J. S.; Chang, F. C. Macromolecules 2002, 35, 8788.
28. Abad, M. J.; Barral, L.; Fasce, D. P.; Williams, R. J. J. Macromolecules 2003, 36, 3128.
29. Liu, Y.; Meng, F.; Zheng, S. Macromol Rapid Commun 2005, 26, 926.
30. Li, H.; Zheng, S. Macromol Rapid Commun 2005, 26, 196.
31. Leu, C. M.; Chang, Y. T.; Wei, K. H. Macromolecules 2003, 36, 9122.
32. Lu, T. L.; Liang, G. Z.; Guo, Z. J Appl Polym Sci 2006, 101, 3652.
33. Lichtenhan, K. D.; Otonari, Y. A.; Carr, M. J. Macromolecules 1995, 28, 8435.
34. Li, C.; Wilkes, G. Chem Mater 2001, 13, 3663.
35. Zeng, Q. H.; Wang, D. Z.; Yu, A. B.; Lu, G. Q. Nanotechnology 2002, 13, 549.
36. Chen, C.; Curliss, D. Nanotechnology 2003, 14, 643.
37. Liu, Y. L.; Chang, G. P. J Polym Sci Part A: Polym Chem 2006, 44, 1869.
38. Chen, W. Y.; Wang, Y. Z.; Kuo, S. W.; Huang, C. F.; Tung, P. H.; Chang, F. C. Polymer 2004, 45, 6897.
39. Ni, Y.; Zheng, S.; Nie, K. M. Polymer 2004, 45, 5557.
40. Liu, Y.; Zhang, W.; Chen, Y.; Zheng, S. J Appl Polym Sci 2006, 99, 927.
41. Liu, Y. H.; Zheng, S. X. J Polym Sci Part A: Polym Chem 2006, 44, 1168.
42. Chen, Q.; Xu, R. W.; Zhang, J.; Yu, D. S. Macromol Rapid Commun 2005, 26, 1878.
43. Zhang, J.; Xu, R. W.; Yu, D. S. Eur Polym Mater 2007, 43, 743.
44. Lee, Y. J.; Kuo, S. W.; Su, Y. C.; Chen, J. K.; Tu, C. W.; Chang, F. C. Polymer 2004, 45, 6321.
45. Lee, Y. J.; Kuo, S. W.; Huang, C. F.; Chang, F. C. Polymer 2006, 47, 4378.
46. Lee, Y. J.; Huang, J. M.; Kuo, S. W.; Chen, J. K.; Chang, F. C. Polymer 2005, 46, 2320.
47. Huang, J. M.; Kuo, S. W.; Lee, Y. J.; Chang, F. C. J Polym Sci Part B: Polym Phys 2007, 45, 644.
48. Sommer, L. H.; Pietrusza, E. W.; Whitmore, F. C. J Am Chem Soc 1947, 69, 2687.
49. Muller, R.; Kohne, F.; Sliwinski, S. J Prakt Chem 1959, 9, 71.
50. Jackson, R. A. Adv Free Chem 1969, 3, 231.
51. Dunkers, J.; Ishida, H. Spectrochim Acta A 1995, 51, 855.
52. Shen, S. B.; Ishida, H. J Polym Sci Part B: Polym Phys 1999, 37, 3257.
53. Agag, T.; Takeichi, T. Macromolecules 2003, 36, 6010.
54. Lin, H. C.; Kuo, S. W.; Huang, C. F.; Chang, F. C. Macromol Rapid Commun 2006, 27, 537.